BJRS

BRAZILIAN JOURNAL
OF
RADIATION SCIENCES
08-03A (2020) 01-18

On the spectral Green's function-constant nodal method for fixed-source S_N problems in X, Y-geometry with arbitrary L'th-order anisotropic scattering

Welton Menezes, Gustavo Alvarez, Ricardo Barros

Fluminense Federal University

wamenezes@id.uff.br

ABSTRACT

Presented here is an extension of the spectral Green's function-constant nodal (SGF-CN) method for the numerical solution of energy multigroup, fixed-source, discrete ordinates (S_N) problems in X, Y-geometry with arbitrary L'th-order of scattering anisotropy, provided L<N. This analytical coarse-mesh method uses the multigroup SGF method for numerically solving the one-dimensional transverse-integrated S_N nodal equations with constant approximations for the transverse leakage terms. The only approximations in the present version of the SGF-CN method occur in these transverse leakage terms, as the energy-group transfer scattering source terms are treated analytically within the offered method. Numerical results to typical model problems are given to illustrate the method's accuracy and to analyze the efficiency of the offered SGF-CN computer code for neutral particle transport calculations.

Keywords: **energy multigroup, fixed source, discrete ordinates, anisotropic scattering.**

ISSN: 2319-0612
Accepted: 2020-12-01

1. INTRODUCTION

A considerable number of phenomena involving neutral particle transport in multiplying and in non-multiplying media can be understood within the deterministic framework of energy multigroup discrete ordinates (S_N) models. In the S_N formulations of particle transport equations in various geometries, the direction-of-motion variables are discretized into a set of distinct numerical values, and angular quadratures are used to approximate the integrals in all angular directions [1].

In addition, one conventionally considers an approximation of the energy-dependent S_N problems, wherein the energy variable is also discretized. Discretization of the energy variable is commonly performed by integrating over G energy groups, leading to the conventional multigroup S_N model, in which the particle energy range is divided into G contiguous energy groups. As with the discretization of the spatial variables, questions regarding efficiency of computer codes have motivated the development of coarse-mesh numerical methods for multigroup S_N problems. By computational efficiency we mean reduced computer running time for fixed accuracy requirements. Among all the currently-known coarse-mesh methods applied to multigroup multidimensional S_N problems, nodal methods are widely regarded as the most accurate [2, 3, 4].

In this paper we describe the multigroup spectral Green's function-constant nodal (SGF-CN) method to numerically solve X,Y-geometry S_N problems in the energy multigroup formulation in non-multiplying media. The only approximations occur in the group leakage terms of the S_N transverse-integrated nodal equations, which are approximated by constants. The SGF-CN method for isotropic scattering carefully analyzed for slab geometry in BARROS and LARSEN [5] and for X,Y-geometry in MENEZES et al. [6]. Here, in the context of X,Y-geometry, we extend the generality of the SGF-CN method by allowing for anisotropic scattering, whereby particles have distinct probabilities of directions of motion after collisions, useful in nuclear technique applications, e.g., Boron Neutron Capture Therapy (BNCT).

An outline of the remainder of this paper follows. In the next section, we describe a spectral analysis [6-8] that we perform in the multigroup transverse-integrated S_N nodal equations to

determine the analytic local homogeneous solution within each discretization node of the spatial grid set up on the rectangular domain. In section 3, we present the offered multigroup SGF-CN method as described in MENEZES et al. [6,9]. Numerical results are given in section 4, and section 5 gives a number of concluding remarks and suggestions for future work.

2. GENERAL SOLUTION OF THE TRANSVERSE-INTEGRATED S_N NODAL EQUATIONS

We begin by considering a spatial grid on a rectangular domain Γ of width X and height Y, where each discretization cell is termed node Γ_{ij} of width h_{x_i} and height h_{y_j} $(i = 1{:}\,I, j = 1{:}\,J)$. Now, on this node, we consider the multigroup X,Y-geometry $\mathrm{S_N}$ equations with a uniform isotropic group interior source Q_g and anisotropic scattering

$$\left[\mu_m \frac{\partial}{\partial x} + \eta_m \frac{\partial}{\partial y} + \sigma_{T_g}\right]\psi_{m,g}(x,y) = \sum_{g'=1}^{G}\sum_{l=0}^{L}\frac{2l+1}{4}\sigma_{S_l}^{g'\to g}\left\{P_l(\mu_m)\phi_{g',l}(x,y) + 2\sum_{k=1}^{l}\frac{(l-k)!}{(l+k)!}P_l^k(\mu_m)\phi_{g',l}^k(x,y)\cos\left(k\varphi_m\right)\sin^k(\theta_m)\right\} + Q_g. \tag{1}$$

The notation is standard [1,10]: $\psi_{m,g}$ is the group angular flux; σ_{T_g} is the group total macroscopic cross section; $\sigma_{S_l}^{g'\to g}$ is the l'th Legendre moment of the differential scattering macroscopic cross section from energy group g' to energy group g; (μ_m, η_m) are the discrete angular directions; $P_l(\mu_m)$ is the l'th Legendre polynomial; $P_l^k(\mu_m)$ is the l'th, k'th associated Legendre polynomial, φ_m is the discrete azimuthal angle and θ_m is the discrete polar angle in the m'th direction, for $m = 1{:}\,M$, where $M = N(N+2)/2$ for the $\mathrm{S_N}$ model; $g = 1{:}\,G$, where G is the total number of groups; and $l = 0{:}\,\mathrm{L}$, where L $(L < N)$ indicates that the Legendre expansion of the differential scattering macroscopic cross section is truncated after $(L+1)$ terms. Moreover, we defined the l'th

Legendre angular moment of the angular flux, $\phi_{g,l}(x,y)$, and the l'th, k'th associated Legendre angular moment of the angular flux, $\phi_{g,l}^{k}(x,y)$, for group g as:

$$\phi_{g,l}(x,y) = \sum_{n=1}^{M} P_l(\mu_n)\psi_{n,g}(x,y)\omega_n, \tag{2}$$

and

$$\phi_{g,l}^{k}(x,y) = \sum_{n=1}^{M} P_l^k(\mu_m)\psi_{n,g}(x,y)\omega_n \cos(k\varphi_m)\sin^k(\theta_m), \tag{3}$$

where ω_n is the angular quadrature weight, $m = 1{:}\,M$.

Tranverse-integrating Eq.(1) separately over the x and the y coordinate directions within node Γ_{ij} and defining the tranverse average angular fluxes of particles migrating in direction (μ_m, η_m) in the g'th energy group

$$\tilde{\psi}_{m,g}(x) = \frac{1}{h_{y_j}} \int_{y_{j-1/2}}^{y_{j-1/2}} \psi_{m,g}(x,y)dy, \tag{4}$$

and

$$\hat{\psi}_{m,g}(y) = \frac{1}{h_{x_i}} \int_{x_{i-1/2}}^{x_{i-1/2}} \psi_{m,g}(x,y)\,dx, \tag{5}$$

and approximating the group transverse leakage terms by their node-edge transverse averages

$$\frac{\eta_m}{h_{y_j}}[\psi_{m,g}(x,y_{j+\frac{1}{2}}) - \psi_{m,g}(x,y_{j-\frac{1}{2}})] \cong \frac{\eta_m}{h_{y_j}}[\hat{\psi}_{m,g,j+\frac{1}{2}} - \hat{\psi}_{m,g,j-\frac{1}{2}}] \equiv \hat{L}_{m,g}, \tag{6}$$

and

$$\frac{\mu_m}{h_{x_i}}[\psi_{m,g}(x_{i+\frac{1}{2}},y) - \psi_{m,g}(x_{i-\frac{1}{2}},y)] \cong \frac{\mu_m}{h_{x_i}}[\tilde{\psi}_{m,g,i+\frac{1}{2}} - \tilde{\psi}_{m,g,i-\frac{1}{2}}] \equiv \tilde{L}_{m,g}, \tag{7}$$

we obtain the transverse-integrated S_N nodal equations, which we write in the general form

$$\Lambda_m \frac{d}{du}\mathfrak{f}_{m,g}(u) + \sigma_{T_g}\mathfrak{f}_{m,g}(u) = \sum_{g'=1}^{G}\sum_{n=1}^{M} S_{m,g}^{n,g'}\mathfrak{f}_{n,g'}(u) + Q_g - \tau_{m,g}, \tag{8}$$

where we have defined: Λ_m=μ_m (or η_m); $u = x$ (or y); $\mathfrak{f}_{m,g}(u) = \tilde{\psi}_{m,g}(x)$ (or $\hat{\psi}_{m,g}(y)$); $\tau_{m,g} = \hat{L}_{m,g}$ (or $\tilde{L}_{m,g}$). We remark that the subscript i,j is dropped to simplify notation. However, we should bear in mind that $(x,y) \in \Gamma_{ij}$. Furthermore, we define

$$S_{m,g}^{n,g'} = \sum_{l=0}^{L} \frac{2l+1}{4} \sigma_{S_l}^{g' \to g} \sum_{k=0}^{l} \frac{2}{(1+\delta_{0k})} \frac{(l-k)!}{(l+k)!} C_{l,m}^{k} C_{l,n}^{k} \omega_n, \tag{9}$$

where

$$C_{l,m}^{k} = \frac{d^k}{d\mu^k} P_l(\mu)|_{\mu=\mu_m} \sum_{n=0}^{k} \frac{k!}{n!\,(k-n)!} \eta_m^n (1-\mu_m^2-\eta_m^2)^{\frac{k-n}{2}} \cos\left(\frac{k-n}{2}\pi\right), \tag{10}$$

with δ_{mn} denoting the Kronecker delta and $n!$ denoting the factorial of a positive integer n.

At this point we solve Eq.(8) in each spatial node Γ_{ij} analytically; therefore we write the expression for the local general solution as

$$\mathfrak{f}_{m,g}(u) = \mathfrak{f}_{m,g}^{h}(u) + \mathfrak{f}_{m,g}^{p}. \tag{11}$$

Here the superscript h denotes the homogeneous solution component and the superscript p denotes the particular solution component of the local general solution.

To obtain the homogeneous solution component $\mathfrak{f}_{m,g}^{h}(u)$, we perform a spectral analysis of Eq.(8) with $Q_g = 0$ and $\tau_{m,g} = 0$ and consider the expression

$$\mathfrak{f}_{m,g,\nu}^{h}(u) = a_k(\nu) \exp\left(-\frac{u-\lambda_\ell}{\nu}\right), \lambda_\ell = \begin{cases} u_{\ell+\frac{1}{2}} & \nu < 0 \\ u_{\ell-\frac{1}{2}} & \nu > 0 \end{cases}, \quad \ell = i(\text{or } j), k = m + (g-1)M. \tag{12}$$

By substituting Eq.(12) into the homogeneous equation corresponding to Eq.(8), we write the result in matrix form as the eigenvalue problem

$$\mathrm{T}^u \mathrm{a}^u(\nu) = \frac{1}{\nu} \mathrm{a}^u(\nu). \tag{13}$$

Here the square matrix T^u of order MG has entries defined by

$$t_{jk}^{u} \equiv \frac{1}{\Lambda_m} \{\delta_{g,g'} \delta_{m,n} \sigma_{T_g} - S_{m,g}^{n,g'}\}, \quad j = m + (g-1)M, m = 1{:}M, g = 1{:}G \text{ and } k = n + (g'-1)M, n = 1{:}M, g' = 1{:}G, \tag{14}$$

where $\delta_{m,n}$ ($\delta_{g,g'}$) is the Kronecker delta. Matrix T^u is a real square matrix, whose eigenvalues ${v_l}^u$ appear in $\pm$ pairs and the corresponding eigenvectors are

$$\begin{gathered} \mathrm{a}^u(v_l) \equiv [a_1(v_l)a_2(v_l) \dots a_k(v_l) \dots a_{MG}(v_l)]^T, \\ k = m + (g-1)M, m = 1{:}\,M, g = 1{:}\,G, l = 1{:}\,MG, \end{gathered} \tag{15}$$

meaning that we have ordered the equations by varying $m = 1{:}\,M$ for each value of g, $g = 1{:}\,G$, to write the eigenvalue problem given in Eq.(13). By solving the eigenvalue problem (13) the homogeneous component of the local general solution appears as

$$\mathrm{f}^h_{m,g}(u) = \sum_{l=1}^{MG} C_l a_k(v_l) \exp\left(-\frac{u-\lambda_\ell}{v_l}\right), k = m + (g-1)M, \tag{16}$$

where $C_l, l = 1{:}\,M$G, are arbitrary constants and $u = x$ (or y) $\in$ Γ_{ij}. Furthermore, spatially constant particular solution of Eq.(8) exists in Γ_{ij} due to uniform group node-interior sources and the constant transverse leakage approximation. Therefore, the particular solution is given by the solution of the linear system

$$\mathrm{A}\mathrm{f}^p = \mathrm{Q}, \tag{17}$$

where the entries of matrix A are given by

$$\begin{gathered} \mathrm{a}_{jk} = \delta_{gg'}\delta_{mn}\sigma_{T_g} - S^{n,g'}_{m,g}, \\ j = m + (g-1)M, m = 1{:}\,M, g = 1{:}\,G, \\ k = n + (g'-1)M, n = 1{:}\,M, g' = 1{:}\,G, \end{gathered} \tag{18}$$

and the transpose of the MG-dimensional column matrix Q is defined by

$$\mathrm{Q} \equiv [Q_1 - \tau_{11} \cdots Q_1 - \tau_{M1} \cdots Q_G - \tau_{1G} \cdots Q_G - \tau_{MG}]^T. \tag{19}$$

Now we substitute Eq.(16) and the solution of Eq.(17) into Eq.(11) to obtain the closed form of the local general solution inside node $\in$ Γ_{ij} for $u = x$ or y.

In the next section we describe a numerical method that preserves these local analytical general solutions for the x and y coordinate directions and uses continuity and boundary conditions to generate numerical solutions to energy multigroup S_N problems in rectangular systems whose spatial grid is composed of many discretization nodes.

3. THE MULTIGROUP SGF-CN METHOD

As we have mentioned, in the present multigroup SGF-CN method, the only approximations occur in the group transverse leakage terms. That is, the one-dimensional multigroup transverse-integrated S_N nodal equations (8) for $u = x$ or y are solved analytically with constant transverse leakage approximations.

Therefore, we consider a spatial grid and integrate Eq.(1) within Γ_{ij}. The result are the classic multigroup spatially discretized S_N balance equations

$$\begin{aligned} &\frac{\mu_m}{h_{x_i}}(\tilde{\psi}_{m,g,i+\frac{1}{2}} - \tilde{\psi}_{m,g,i-\frac{1}{2}}) + \frac{\eta_m}{h_{y_j}}(\widehat{\psi}_{m,g,j+\frac{1}{2}} - \widehat{\psi}_{m,g,j-\frac{1}{2}}) + \\ &\sigma_{T_g}\overline{\psi}_{m,g} = \sum_{g'=1}^{G}\sum_{n=1}^{M} S_{m,g}^{n,g'}\overline{\psi}_{n,g'} + Q_g, g = 1{:}\,G, m = 1{:}\,M. \end{aligned} \tag{20}$$

Here we have defined the group node-average angular flux ($\bar{\psi}_{m,g}$) which, for $u = x$ in Eq.(8), is related to the multigroup node-edge average angular fluxes in the incoming directions and to the multigroup node-interior source and transverse leakages as

$$\begin{aligned} \overline{\psi}_{m,g} = &\sum_{\mu_n>0}\sum_{g'=1}^{G}\chi_{n,g'\to m,g}\tilde{\psi}_{n,g',i-\frac{1}{2}} + \sum_{\mu_n<0}\sum_{g'=1}^{G}\chi_{n,g'\to m,g}\tilde{\psi}_{n,g',i+\frac{1}{2}} + \\ &\widehat{G}_{m,g}(Q_1, Q_2, \cdots, Q_G), m = 1{:}\,M, g = 1{:}\,G. \end{aligned} \tag{21}$$

Equation (21) is referred to as the multigroup SGF-CN auxiliary equations, where $\chi_{n,g'\to m,g}$ and $\widehat{G}_{m,g}(Q_1, Q_2, \cdots, Q_G)$ are determined by requiring that the local general solution of Eq.(8) with $u = x$ have group node-average and node-edge average angular fluxes that for all values of C_l satisfy Eq.(21). Therefore, we first evaluate the group node-average and node-edge average angular

fluxes that correspond to the local general solutions given by combining Eq.(16), with $u = x$, and the solution of Eq.(17); then we use these in Eq.(21) by requiring that the result hold for all choices of C_l. As a result, we find

$$\widehat{G}_{m,g}(Q_1, Q_2, \cdots, Q_G) = \tilde{\psi}^p_{m,g} - \sum_{n=1}^{M} \sum_{g'=1}^{G} \chi_{n,g' \to m,g} \tilde{\psi}^p_{n,g'}. \tag{22}$$

Moreover, the constants $\chi_{n,g' \to m,g}$ must satisfy

$$\frac{a^x_{m,g}(\nu_\ell)}{\mathcal{L}^x_\ell}\{\exp(\mathcal{L}^x_\ell) - 1\} = \exp(\mathcal{L}^x_\ell) \sum_{\mu_n > 0} \sum_{g'=1}^{G} \chi_{n,g' \to m,g} a^x_{n,g'}(\nu_\ell) + \sum_{\mu_n < 0} \sum_{g'=1}^{G} \chi_{n,g' \to m,g} a^x_{n,g'}(\nu_\ell), \nu_\ell > 0, \tag{23}$$

and

$$\frac{a^x_{m,g}(\nu_\ell)}{\mathcal{L}^x_\ell}\{\exp(\mathcal{L}^x_\ell) - 1\} = \sum_{\mu_n > 0} \sum_{g'=1}^{G} \chi_{n,g' \to m,g} a^x_{n,g'}(\nu_\ell) + \exp(\mathcal{L}^x_\ell) \sum_{\mu_n < 0} \sum_{g'=1}^{G} \chi_{n,g' \to m,g} a^x_{n,g'}(\nu_\ell), \nu_\ell < 0, \tag{24}$$

where we have defined $\mathcal{L}^x_\ell = h_{x_i}/|\nu_\ell|$.

At this point we note that Eqs.(23-24) form a system of M^2G^2 linear algebraic equations for the M^2G^2 unknowns $\chi_{n,g' \to m,g}$. By solving this system for $\chi_{n,g' \to m,g}$, Eq.(21) constitutes the auxiliary equations which, with the conventional multigroup S_N balance equations (20), are exactly satisfied by the general solution of the one-dimensional transverse-integrated S_N nodal equation (8) with $u = x$. A similar auxiliary equation holds for Eq.(8) with $u = y$ and appears as

$$\overline{\psi}_{m,g} = \sum_{\eta_n > 0} \sum_{g'=1}^{G} \theta_{n,g' \to m,g} \widehat{\psi}_{n,g',j-\frac{1}{2}} + \sum_{\eta_n < 0} \sum_{g'=1}^{G} \theta_{n,g' \to m,g} \widehat{\psi}_{n,g',j+\frac{1}{2}} + \tilde{G}_{m,g}(Q_1, Q_2, \cdots, Q_G), m = 1{:}M, g = 1{:}G. \tag{25}$$

In conclusion, the multigroup spatially discretized S_N balance equation (20) together with auxiliary equations (21) and (25) and appropriate continuity and boundary conditions form the

multigroup SGF-CN equations. The SGF-CN equations are then solved iteratively by performing "node-block inversions" described in references [6-9]. This iterative scheme uses the most recent estimates for the incoming multigroup node-edge average angular fluxes for each node to completely solve the S_N problem in that node and obtain estimates for the outgoing multigroup node-edge average angular fluxes that are used as incoming fluxes for the adjacent discretization nodes of the spatial grid in the directions of the transport sweeps.

In the next section we consider two model problems to illustrate the accuracy of the present multigroup SGF-CN method for deep penetration problems.

4. RESULTS AND DISCUSSION

At this point we present numerical results to two fixed-source model problems using level symmetric (LQ_N) angular quadrature sets [1,10] and stopping criteria requiring that the discrete maximum norms of the relative deviations between two consecutive estimates of the multigroup node-edge average scalar fluxes be no greater than a prescribed positive number ϵ. In order to compare the solutions obtained by the offered method with reference values, we use the percentage relative deviations that we estimate as $\varepsilon = \left(\frac{V_r - V}{V_r}\right) \times 100$, where V_r is the reference quantity and V is the quantity generated by the SGF-CN method. Moreover, the conventional linear nodal method (LN) with the source iteration (SI) scheme [1,4] was also programed for a consistent comparison.

4.1. Forward-scattering 2-D shield problem

The problem considered here, proposed in Benchmark Problem Committee [12], simulates a realistic shielding structure. This two-energy group test problem consists of a uniform isotropic neutron source stored in a highly absorbing shielding material. The geometry is a homogeneous system (133 cm × 140 cm). The source emits neutrons whose energy range has been divided into two energy groups, i.e., $Q_1 = 0.006546$ and $Q_2 = 0.017701$ neutrons/cm^{3}sec. The macroscopic cross sections for the homogeneous domain are given in reference [12]. Results in this isotropic scattering problem can be found in [6, 12]. Adding the forward scattering cross sections $\sigma_{S_l}^{1\to 1} =$

0.008976, $\sigma_{S_l}^{2\to 2} = 0.003914$ and $\sigma_{S_l}^{1\to 2} = 0.009016$ for all l [12], this isotropic scattering problem can be transformed into "equivalent" anisotropic scattering problem as discussed in ROY [13]. The converted macroscopic cross sections for the homogeneous domain are given in Table 1. The numerical experiment is the estimate of neutron leakage $\tilde{\mathbb{J}}_g^T = \frac{1}{4}\sum_{j=1}^{J}\sum_{\mu_n>0}\left(\mu_n\tilde{\psi}_{n,g,I+1/2,j}h_{y_j}\omega_n\right)$, $g = 1{:}2$ through the whole physical boundary on the right-hand side of the structure, i.e., $\{(x,y)|\, x = 133 \;\; and \; 0 \le y \le 144\}$.We solved this problem using the present multigroup SGF-CN method with the NBI iteration scheme, level symmetric S_{12} and S_{20} angular quadrature sets [1,10] and the stopping criterion with $\epsilon = 10^{-6}$. Moreover, we considered the P_n $(n = 1, 3, \cdots, 11)$ truncated expansions of the anisotropic scattering. In this way the well-validated isotropic scattering version of the code SGF-CN [6] is used to validate the anisotropic version.

Table 2 displays the percentage relative deviations of the results generated for $\tilde{\mathbb{J}}_g^T, g = 1{:}2$, of the corrected problem with respect to the version of the isotropic problem by the present SGF-CN method. Our numerical experiment consists of generating two-group leakages with S_{12} and S_{20} models, which deviate from the reference results less than 5%. As we see in Table 2, all P_n scattering models, except P_1, converged satisfactory, mainly for the fast group leakage, on a spatial grid composed of 27×28 nodes. The transport correction did not provide good approximations for the linearly anisotropic scattering test; this contradicts the fact that this problem is highly absorbing (total right leakage $\sum_{g=1}^{2}\tilde{\mathbb{J}}_g^T \approx 4.2701 \times 10^{-4}$) and theoretically low dependent of scattering. As noted in YAMAMOTO et al. [14], there are possibly physics ambiguities or the used transport corrected macroscopic cross sections are not mathematically consistent, a topic that has to be looked at in the future.

Figure 1 displays the profile of the scalar fluxes for the two energy groups. Also shown are the relative percentage deviations for P_n $(n = 1, 3, \cdots, 11)$ with respect to the original isotropic problem. The scalar fluxes generated at $y = 80$ cm were computed using a discretization grid with 756 nodes and S_{20} quadrature. From Figure 1, significant differences are not seen with increasing anisotropy order. However, Figures (2.a) and (2.b) indicate that the magnitudes of the relative deviations increase as it one moves away from the boundary.

Table 1: Macroscopic cross-section (cm^{-1}) for the transformed anisotropic shield problem.

Group	σ_T^g	σ_A^g	$\sigma_{S_0}^{g\to g}$	$\sigma_{S_0}^{g-1\to g}$	$l>0$	
					$\sigma_{S_l}^{g\to g}$	$\sigma_{S_l}^{g-1\to g}$
1	1.10108E-1[a]	6.1723E-2	6.9470E-3	-	8.9760E-3	-
2	1.08529E-1	9.6027E-2	4.8500E-3	2.3434E-2	3.9140E-3	9.0160E-3

[a] read as 1.10108×10^{-1}.

Table 2: Percentage deviations of total right leakages of SGF-CN calculations for problem No. 1

LQ_N	**12**	**20**	**12**	**20**
g	$\tilde{J}_g^T$ **Reference**[a]			
1	5.48328E-04	5.48131E-04		
2	8.78682E-04	8.78352E-04		
	P_1[c]		**P_3**	
1	1.7320E+01[b]	1.7324E+01	-3.5280E-01	-3.6756E-01
2	1.2784E+01	1.2791E+01	-4.3196E+00	-4.3304E+00
	P_5		**P_7**	
1	5.5149E-02	5.9785E-02	2.9727E-03	1.0144E-02
2	-3.9987E+00	-3.9915E+00	-4.0443E+00	-4.0353E+00
	P_9		**P_{11}**	
1	-1.0578E-03	-2.0305E-02	-7.8055E-03	-7.9333E-01
2	-4.0480E+00	-4.0650E+00	-4.0539E+00	-4.8117E+00

[a] results generated using the isotropic version of the shield problem (see reference [6]).

[b] read as $1.7320\times10^{+1}$;

[c] P_n: indicates that the scattering macroscopic cross section was truncated after the n'th term;

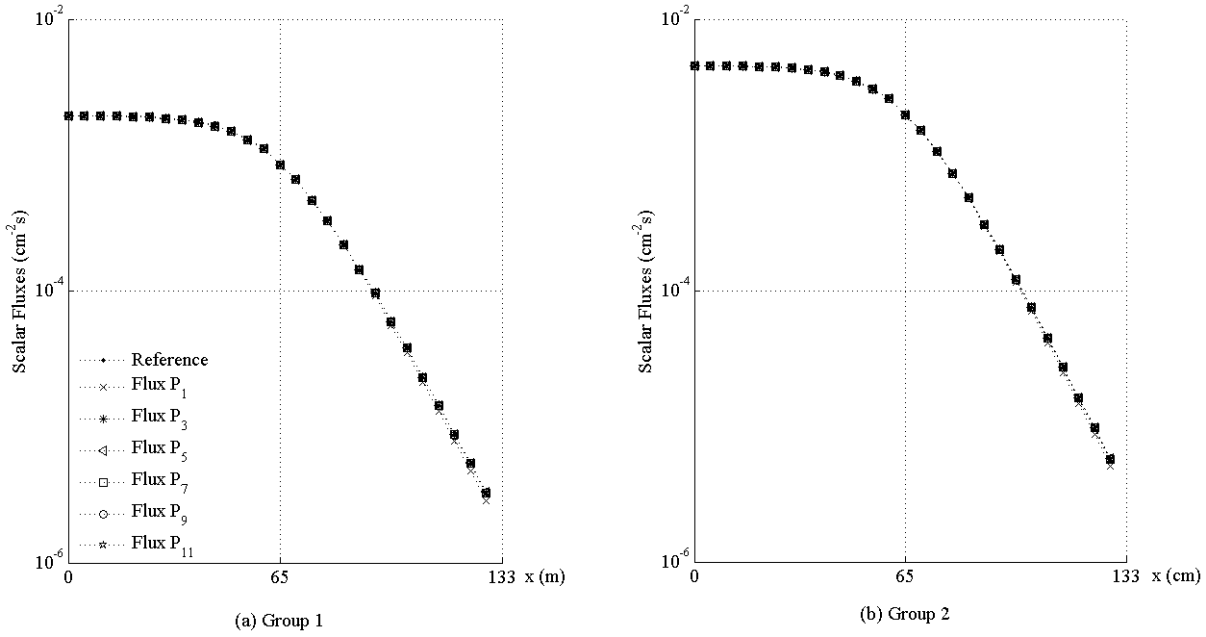

Figure 1: *Scalar flux profiles for groups 1 and 2 at y=80cm for Problem No. 1*

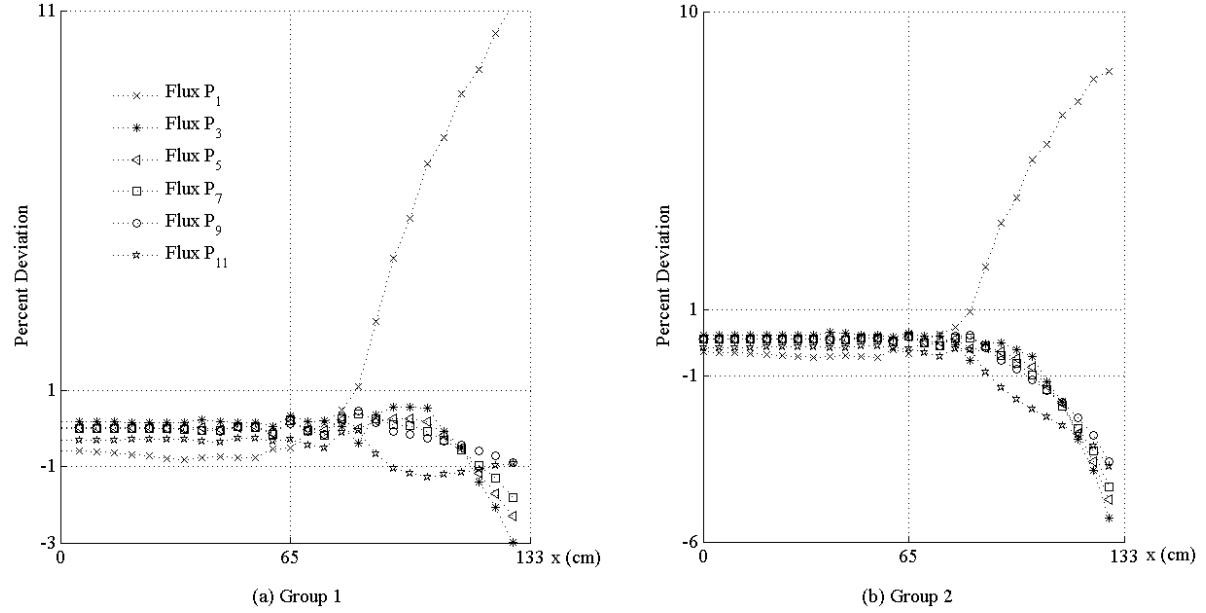

Figure 2: *Relative percentage deviations of scalar fluxes with respect to the isotropic problem.*

4.2. Oil well-logging problem

The problem considered here is illustrated in Figure 3 and mocks-up a seven energy group version of the oil well logging problem considered in [4, 5, 6, 7]. The group macroscopic cross sections are listed in Table 3.

Our numerical experiment consists of estimating the absorption rate per unit length of the z-coordinate direction within the neutron detector region (Figure 3). To solve this problem, we consider different parameters for the seven energy-group S_{12} model in X,Y-geometry, including scattering orders (P_0, P_1, and P_3), and mesh refinements. As reference results, we use the ones generated by the conventional LN method with the source iteration (SI) scheme [1] on a spatial grid composed of 112 discretization cells in the x direction and 128 cells in the y direction, and 3'rd order scattering anisotropy. Table 4 displays the relative percentage deviations of total absorption rate densities ($\delta D_R^T,\ R = 1,2$) in the neutron detector regions of Figure 3 with respect to the reference solution, which was generated by the conventional LN method on a spatial grid composed of square nodes of 0.5 cm side. As we see, for fine spatial grids, the relative deviations of the detector responses, with respect to the finest grid LN reference results, are less than 5%. As the spatial grids coarsen, the numerical results deviate from the reference results. Moreover, we remark that total absorption rate densities increase with increasing scattering anisotropy. The results indicate that the third order scattering is necessary to solve this problem. Also, the number of iterations for the SGF-CN method with the NBI scheme to generate results with relative deviations less than 1% was roughly six times smaller than the number of iterations for the LN method with the SI scheme to converge this problem with relative deviations also less than 1%, with the same stopping criterion, using $\epsilon = 10^{-5}$.

Table 3: Seven group macroscopic cross-sections (cm^{-1}) for the oil well-logging problem

zone	1		2		3	
$\boldsymbol{g}$	$\boldsymbol{\sigma_{T_g}^z}$	$\boldsymbol{\sigma_{S_{0,z}}^{g\to g}}$	$\boldsymbol{\sigma_{T_g}^z}$	$\boldsymbol{\sigma_{S_{0,z}}^{g\to g}}$	$\boldsymbol{\sigma_{T_g}^z}$	$\boldsymbol{\sigma_{S_{0,z}}^{g\to g}}$
1	0.830263	0.314419	1.194676	0.634883	1.011091	0.494460
2	0.7	0.5	0.752375	0.5	0.81519	0.5

	Zones 1, 2 and 3						
$\boldsymbol{g}$	$\boldsymbol{\sigma_S^{g\to g}}$			$\boldsymbol{\sigma_S^{g\to g+1}}$			
	σ_{S_1}	σ_{S_2}	σ_{S_3}	σ_{S_0}	σ_{S_1}	σ_{S_2}	σ_{S_3}
1	0.3	0.2	$3/35$	0.5	0.3	0.2	$3/35$
2	0.3	0.2	$3/35$	-	-	-	-

$$\sigma_{T_g}^z = \left(\frac{z+20}{21}\right)^5 \left(\frac{g}{10}\right) - 0.15\delta_{g,5},\ z = 1{:}\,3 \text{ and } g = 3{:}\,7,$$

$$\sigma_{S_{l,z}}^{g\prime\to g} = \left(\frac{z+20}{21}\right)\left(\frac{g\prime}{100(g-g'+1)}\right)\left(0.7 - \frac{g+g\prime}{200}\right)^l, g' = 1{:}\,g, g = 3{:}\,7, l = 1{:}\,3, z = 1{:}\,3.$$

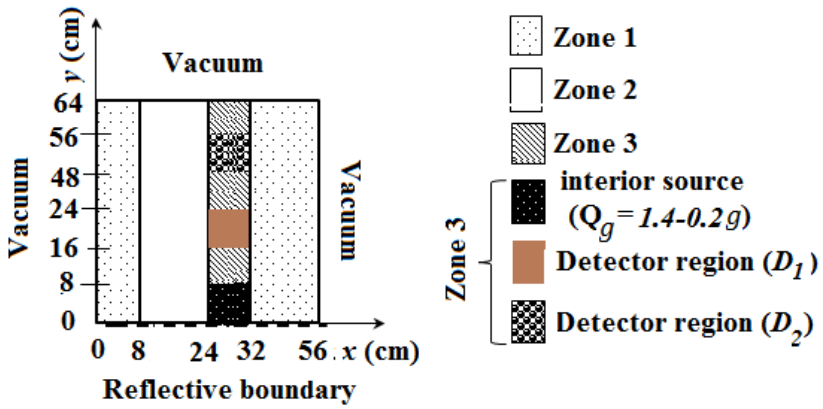

Figure 3: *The geometry of the oil well-logging problem.*

Table 4: Relative Percentage deviations of total absorption rate densities of SGF-CN and LN results for problem No. 2

h_u [a] cm	Method	P_3 [b]			P_1			P_0		
		δD_1^T	δD_2^T	# it.[c]	δD_1^T	δD_2^T	# it.[c]	δD_1^T	δD_2^T	# it.[c]
4	SGF-CN	23.51	-14.33	10	29.31	15.74	11	75.44	81.05	17
	LN	1.56	12.71	86	6.74	38.21	93	64.44	89.03	79
2	SGF-CN	6.57	-6.32	12	12.94	22.64	13	68.98	83.36	19
	LN	0.06	1.08	95	6.79	28.64	92	66.67	85.48	95
1	SGF-CN	1.85	-2.09	15	8.42	26.18	16	67.26	84.64	23
	LN	-0.00	0.07	86	6.68	27.95	88	66.57	85.28	101

[a] h_u $u = x$ (or y): mesh width (or height);

[b] P_n: indicates that the scattering macroscopic cross section was truncated after the n'th term;

[c] # it.: number of iterations to reach the stopping criterion;

h_u = 0.5-cm mesh LN results: D_1^T =1.46513× 10^{-1} and D_2^T = 9.21370× 10^{-8}.

5. CONCLUSION

The SGF-CN method for monoenergetic S_N problems in X,Y-geometry were originally described in BARROS et al. [8]. In this paper, we have described a generalization of the application of the SGF-CN method [6, 8, 9] to energy multigroup, fixed-source, S_N problems in X,Y-geometry with linearly anisotropic scattering. This generalization was straightforward, since it was not necessary to change significantly the conventional SGF-CN method; the only modification is that the term of the scattering source became more and more dependent on the direction of motion. This extension is the most signicant contribution of this paper.

The results for the two model problems considered in the previous section are very accurate with respect to the results reported in [6, 8, 9, 14, 15]. The offered method is very accurate for coarse-mesh calculations, even though we have considered flat approximations for the group leakage terms in the transverse-integrated S_N nodal equations. In addition, the SGF-CN results turned out to be as accurate as the conventional LN results, without the need of using the balance equations for the first order spatial moments.

In the future, we intend to consider exponential [14] and linear [15] approximations for the transverse-leakage terms in the S_N multigroup models, so as to improve the accuracy of the numerical results in coarse-mesh calculations. As mentioned earlier, the reason for the high accuracy of the class of spectral nodal methods for coarse-mesh S_N deep penetration problems is that the only approximation involved is the approximation for the transverse leakage terms in the one-dimensional transverse-integrated S_N nodal equations. Moreover, the use of the NBI scheme with the present SGF-CN method was much more efficient than the use of the SI scheme with the LN method, as the former generated accurate results in fewer iterations than the latter. A drawback of the offered multigroup SGF-CN method with NBI iterations is that the group node-edge average angular fluxes must be stored, whereas with the SI scheme, only the group cell-average scalar fluxes must be stored for isotropic scattering. Also the multigroup SGF-CN method, as described in this paper, requires fairly costly matrix calculations, before the beginning of the NBI iteration process. These are the solution of one (M×G)-order eigenvalue problem for each material zone of the domain, and the solution of M×G linear systems of order M×G for each region. In the future, we intend to alleviate these negative features by using acceleration strategies to the NBI scheme, besides implementing parallelization architecture for both the solution of eigenvalue problems and

for the solution of the linear systems on independent processors. We also intend to extend the arbitrary anisotropic scattering, multigroup SGF-CN method for X,Y,Z-geometry problems [16].

ACKNOWLEDGMENT

The authors wish to thank the following for their financial support: CNPq - Conselho Nacional de Desenvolvimento Científico e Tecnológico, Brazil and FAPERJ - Fundação Carlos Chagas Filho de Amparo à Pesquisa do Estado do Rio de Janeiro, Brazil.

REFERENCES

[1] LEWIS, E, E., MILLER, W. F. **Computational methods of neutron transport**, 2nd ed. La Grange Park, Illinois: American Nuclear Society, 1993.

[2] WALTERS, W. F.; O'DELL, R. D. A nodal methods for discrete-ordinates transport problems in x,y-geometry. **Proceedings of the International Topical Meeting on Advances in Mathematical Methods for the Solution of Nuclear Engineering Problems**. vol. 1, Munich: American Nuclear Society, 1981. pp. 115-129.

[3] LAWRENCE, R. D. Progress in nodal methods for the solution of the neutron diffusion and transport equations. **Progress in Nuclear Energy**, vol. 17, pp. 93-116, 1986.

[4] AZMY, Y. Y. Comparison of three approximations to the linear-linear nodal transport method in weighted diamond-difference form. **Nuclear Science and Engineering**, pp. 190-200, 1988.

[5] BARROS, R. C.; LARSEN E. W. A numerical method for multigroup slab-geometry discrete ordinates problems with no spatial truncation error. **Transport Theory and Statistical Physics**, pp. 441 - 462, 1990.

[6] MENEZES, W. A. et al. An analytical nodal method for energy multi-group discrete ordinates transport calculations in two-dimensional rectangular geometry, **International Journal of Nuclear Energy Science and Technology**, pp. 66 – 80, 2018.

[7] DOMINGUEZ, D. S.; HERNANDEZ, R.G., BARROS, R. C. Spectral nodal method for numerically solving two-energy group x,y geometry neutron diffusion eigenvalue problems. **International Journal of Nuclear Energy Science and Technology**, 2010.

[8] BARROS, R. C.; LARSEN E. W. A spectral nodal method for one-Group X,Y-geometry discrete ordinates problems. **Nuclear Science and Engineering**, pp. 34-45, 1992.

[9] MENEZES W. A.; ALVAREZ G. B.; BARROS R. C. A generalization of the energy multigroup spectral Green's function constant nodal method for fixed-source S_N problems in x, y-geometry with arbitrary l'th-order of anisotropic scattering, In: **INTERNATIONAL NUCLEAR ATLANTIC CONFERENCE**, 2019, Santos. On CD Proceedings.

[10] CACUCI, D. G. Handbook of nuclear engineering, Vol. I: **Nuclear Engineering Fundamentals.** New York: Springer Science + Business Media LLC, 2010.

[11] Benchmark Problem Committee of the Mathematics and Computation Division of Amer. Nucl. SOC:. Argonne Code Center; **Benchmark problem book, numerical determination of the space, time, angle or energy distribution of particles in an assembly**, ANL-7416, 1972.

[12] ROY, R. Anisotropic scattering for integral transport codes. Part 2. Cyclic tracking and its application to xy lattices. **Annals of Nuclear Energy**, pp. 511-524, 1991.

[13] YAMAMOTO, A. et al. Simplified treatments of anisotropic scattering in LWR core calculations. **Journal of Nuclear Science and Technology**, pp. 217-229, 2008.

[14] MELLO, J. M.; BARROS, R. C. An exponential spectral nodal method for one-speed x,y-geometry deep penetration discrete ordinates problems". **Annals of Nuclear Energy**, pp. 1855 - 1869, 2002.

[15] DOMINGUEZ, D. S.; BARROS, R. C. The spectral Green s function linear-nodal method for one-speed x, y-geometry discrete ordinates deep penetration problems. **Annals of Nuclear Energy**, pp. 958 - 966, 2007.

[16] ANLI, F.; GÜNGÖR, S. A spectral nodal method for one-group x,y,z-Cartesian geometry discrete ordinates problems. **Annals of Nuclear Energy**, pp. 669 - 680, 1996.